Structure and Thermal Stability of Photosystem II Reaction Centers Studied by Infrared Spectroscopy†

Javier De Las Rivas*,‡ and James Barber§

Department of Biochemistry and Molecular Biology, Faculty of Science, University of the Basque Country, P.O. Box 644, E48080 Bilbao, Spain, and Department of Biochemistry, Imperial College of Science, Technology & Medicine, London SW7 2AY, U.K.

Received March 24, 1997; Revised Manuscript Received May 20, 1997⊗

ABSTRACT: The secondary structure of photosystem II reaction centers isolated from pea has been deduced from quantitative analysis of the component bands of the infrared amide I spectral region, determined by FTIR spectroscopy. The analysis shows the isolated complex to consist of 40% α-helix, 10% β-sheet, 14% β-strands (or extended chains), 17% turns, 15% loops, and 3% nonordered segments. These structural protein elements were determined for samples in H_2O, in D_2O, and in dried films. The isolated reaction center, composed of proteins D1,D2,cytochrome b_{559}, and *Psb*I, has been predicted to contain a total of 13 transmembrane α-helices, which conveys a percentage of this type of structure congruent with the structural determination deduced from FTIR spectra. The process of thermal destabilization of the reaction centers has also been studied by FTIR spectroscopy, showing a clear main conformational transition at 42 °C, which indicates a high thermal sensitivity of the secondary structure of this protein complex. Such thermal instability may correlate with the well-described high sensitivity of photosystem II to damage and may relate to the process of rapid protein degradation that photosystem II suffers during *photoinhibition* of plants.

Photosystem II (PSII)[1] is an integral membrane protein complex that uses light energy to split water, producing free molecular oxygen plus protons and electrons. The electrons feed a series of redox reactions ending in the reduction of plastoquinone (final electron acceptor of the complex) (Barber, 1994). The reaction center (RC) of this protein complex is where the primary photosynthetic redox events occur and when isolated consists of five different polypeptides called D1 protein (38 kDa MW), D2 protein (39.5 kDa MW), cytochrome b_{559} (subunits a and b, 9.3 and 4.4 kDa MW) and PsbI protein (4.2 kDa MW) [MW for pea from Swiss-Prot database (1996)].

Since 1985, when the first atomic resolution structure of an integral membrane protein was described (Deisenhofer et al., 1985), a small number of membrane protein structures have been solved (Walker & Saraste, 1996). Difficulties in the isolation, purification, and crystallization of membrane proteins are the main technical obstacles. To date, detailed structures of only seven families of integral membrane proteins are known, and five of them are involved in respiration and photosynthesis, including two photosynthetic RCs: the RC from purple bacteria (Deisenhofer et al., 1985; Allen et al., 1987) and the photosystem I RC from cyanobacteria (Krauss et al., 1993). Despite this progress in the field in the last decade, the three-dimensional (3D) structure of the PSII protein complex has not yet been determined due to the lack of 3D crystals of sufficient stability and size needed for high-resolution X-ray spectroscopy. Some 2D crystals of PSII have been obtained and studied by electron microscopy, but from these preparations, only 2D projection maps of the whole PSII complex have been achieved (Dekker et al., 1990; Lyon et al., 1993; Nicholson et al., 1996; Tsiotis et al., 1996; Nakazato et al., 1996; Marr et al., 1996). Other analogous studies searching for the elucidation of the 3D architecture of PSII have only produced low-resolution 3D images of the complex (Holzenburg et al., 1993; Santini et al., 1994; Boekema et al., 1995). Very little is therefore known about the secondary structure of PSII RCs. The lack of direct structural information about PSII makes the use of other spectroscopic methods, which only need isolated protein complexes in solution, very valuable.

Infrared (IR) spectroscopy has shown its potential in the elucidation of protein conformation (Haris & Chapman, 1993; Arrondo et al., 1993), and in spite of its present limitations at the level of structural resolution, it can be applied successfully to characterize the secondary structure of soluble and membrane proteins, even for the case of protein complexes having large molecular masses with high structural complexity. The infrared amide I band in the 1600−1700 cm^{-1} region, arising mainly from carbonyl (C═O) stretching vibrations of the peptide bond (Krimm & Bandekar, 1986), is conformationally sensitive and is the region most commonly used in structural studies of proteins (Surewicz & Mantsch, 1988). The recent advances in Fourier transform infrared (FTIR) instrumentation and computer software for spectral analyses have dramatically widened the possibilities of quantitative IR spectroscopy which clearly

† This work was supported by funds from the University of the Basque Country (Grants 042.123-EA202/93 and EA095/94) and by the Biotechnology and Biological Sciences Research Council (BBSRC, U.K.).

* Corresponding author. Phone: 34-4-464 7700 (extensions 2407 or 2567). Fax: 34-4-464 8500. E-mail: gbpdesaj@lg.ehu.es.

‡ University of the Basque Country.

§ Imperial College of Science, Technology & Medicine.

⊗ Abstract published in *Advance ACS Abstracts,* July 1, 1997.

[1] Abbreviations: FTIR, Fourier transform infrared; IR, infrared; MW, molecular mass; PSII, photosystem II; RC, reaction center; 3D, three-dimensional; 2D, two-dimensional.

S0006-2960(97)00684-3 CCC: $14.00

improves the structural information obtained (Arrondo et al., 1993). Finally, a combination of structural analysis and thermal denaturation studies of several samples in buffers (containing H_2O or D_2O) and in dried films has demonstrated a very good way to obtain the best information from IR spectroscopy of proteins (Arrondo et al., 1994; Bañuelos et al., 1995; Taneva et al., 1995).

Isolated photosystem II reaction centers have been previously studied by FTIR (He et al., 1991). The structural determination in that work was done by a quantification method based on factor analyses and multiple linear regression, which implies comparison with a set of standard proteins of known structure (18 proteins, most of them water-soluble) (Lee et al., 1990). That method does not permit the assigment of the specific bands found in the IR spectra of the protein studied and only allowed a general determination of three kinds of protein structural elements: α-helix, *β*-sheets, and turns. We now present a more complete quantitative determination of the secondary structure of PSII RCs based on a new analysis of its IR spectra in H_2O, D_2O, and films. We use a powerfull method of analysis of FTIR spectra which has been recently applied successfully to the structural study of other important integral membrane proteins like cytochrome *c* oxidase (Arrondo et al., 1994; Echabe et al., 1995). In this paper, we also examine the thermal behavior of the PSII RC using FTIR spectra recorded over the 20−80 °C temperature range. The FTIR profile of the thermal denaturation of the PSII RC complex revealed a clear conformational transition which seems to be related to a functional inactivation of this protein complex.

MATERIALS AND METHODS

Sample Preparation. Reaction centers of PSII were isolated from pea (*Pisum sativum*) according to Chapman et al. (1988). Samples for FTIR spectroscopy were prepared in buffer consisting of 10 mM phosphate (pH 7.0) with 2 mM dodecyl maltoside. The protein concentration was ≈30−40 mg/mL (which is about 0.32−0.42 mM for an estimated MW of the PSII RCs of 95 kDa). The samples in D_2O were obtained by exchange, using Centricon-100 tubes (Amicon Inc.), to an equivalent D_2O buffer: 10 mM phosphate (pD 7.0) with 2 mM dodecyl maltoside. To produce dried films, a preparation was spread onto the FTIR sample window and slowly dried in the dark under vacuum. The samples were located in a thermostatted cell between two windows, one of calcium fluoride (CaF_2, 25 mm × 2 mm) (Wilmad Glass Co. Inc.) and another of germanium (Ge, 25 mm × 3 mm) (Davin Optical Ltd., Barnet-Herts, U.K.) with a path length spacer of 6 *μ*m (12 *μ*m for the samples in D_2O) (Harrick Scientific Co.). The germanium window was placed facing the IR source, as a filter to cut out the red He-Ne laser colinear with the IR beam and to prevent any undesirable actinic effects on the PSII RCs.

Infrared Spectroscopy Analyses. Spectra were acquired in a Nicolet 520 spectrometer equipped with a MCT detector. Typically, 500 scans for each, background and sample, were collected and the spectra obtained with a nominal resolution of 2 cm^{-1}. Protein samples and buffer controls were measured one after the other with identical scanning parameters. The removal of the solvent signal was done by subtraction of the IR spectra of the buffer from the spectra of each sample within the 1900−1400 cm^{-1} region. The frequency of the water bending mode has a highly dominating absorption in the 1660−1620 cm^{-1} region, which overlaps with the amide I protein vibrational band (Arrondo et al., 1993). An adequate removal of the water band was done by subtracting till a flat baseline in the 1900−1750 cm^{-1} region was achieved, where the water still absorbs but is free from any protein absorbance. This was equivalent to eliminating the specific band for water at 2125 cm^{-1} (Arrondo et al., 1993). Data treatment and band decomposition of the original amide I have been described elsewhere (Arrondo et al., 1989, 1993, 1994; Bañuelos et al., 1995; Echabe et al., 1995). Decomposition of the original amide I band in H_2O and D_2O media into its constituents improves the assignment of the component bands to specific structural features (Arrondo et al., 1994). Briefly, for each component four parameters are considered: band position, band height, band width, and band shape. Thus, in a typical amide I band decomposition with around eight band components, the number of parameters is about 32. The number and initial position of the component bands were obtained through Fourier deconvolution and derivation. Initial heights were set at 90% of those in the original spectrum for the bands in the wings and for the most intense component and at 70% of the original intensity for the other bands. Initial band widths were estimated from the Fourier derivative. The Lorentzian component of the bands was initially set at 10%. The baseline was corrected to zero prior to starting the fitting process. The curve fitting by iteration procedure was carried out in three steps as described in Arrondo et al. (1994). This method uses the software SpectraCalc (Galactic Inc., Salem, NH). The mathematical solution to the decomposition may not be unique, but if restrictions are imposed such as the maintenance of the initial band positions in an interval of ±1 cm^{-1}, the preservation of the bandwidth within the expected limits or the agreement with theoretical boundaries or predictions, the result becomes, in practice, unique. The results are verified by constructing artificial curves with the parameters obtained and performing the band decomposition on those, with identical outcomes. The quantification procedure has an estimated error of ≤3% (Arrondo et al., 1994; Bañuelos et al., 1995). The method has been used successfully with other well-characterized membrane proteins (Arrondo et al., 1994; Echabe et al., 1995).

Thermal Treatments. To study the effect of temperature, samples in H_2O and in D_2O buffers were heated in steps of around 3 °C, through the 20 to 80 °C interval. The temperature was monitored by a thermocouple probe placed in contact with the edge of the IR window. After each heating step, the sample was left to stabilize for 5 min and the corresponding spectrum recorded. After the spectra were recorded, the interferograms were processed by ratioing with respect to the background and the resulting IR spectra were treated as described above.

RESULTS

Structure of Photosystem II Reaction Centers from Amide I Band Decomposition. The structural data of isolated PSII RCs have been obtained from the conformationally sensitive infrared spectral amide I band arising from the peptide bond (Arrondo et al., 1993). Figure 1 displays the decomposed amide I band contours of the PSII RCs in H_2O media, in D_2O media, and in dried films. The peak position and percentage area obtained for each band are shown in Table 1. The spectra of PSII RCs in H_2O and in D_2O exhibit eight

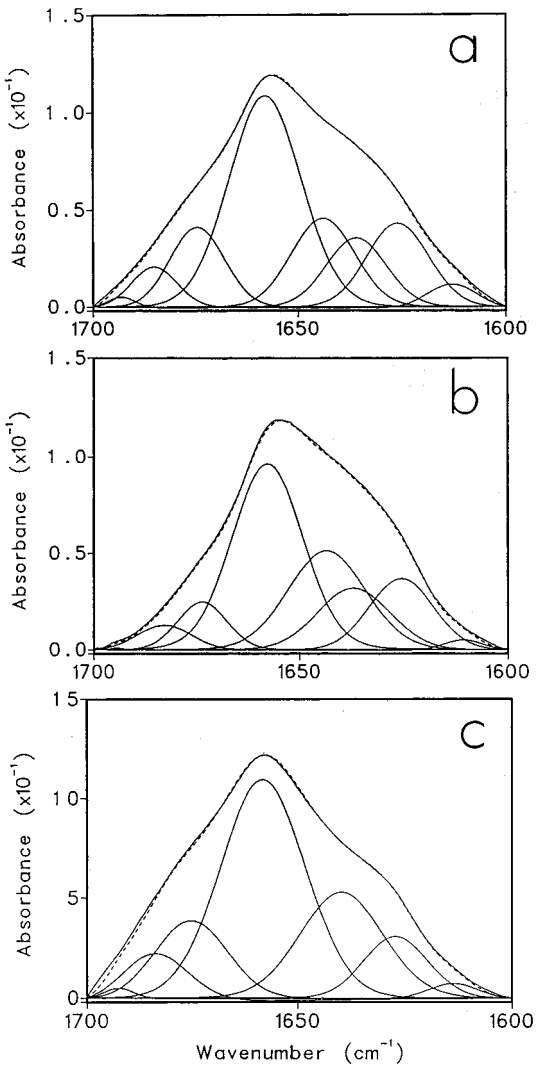

FIGURE 1: Band decomposition of the original amide I band at 25 °C of the PSII RCs in H_2O buffer (a), in D_2O buffer (b), and in dried films (c). The spectra were baseline corrected prior to the decomposition procedure. The numerical values obtained are reflected in Table 1. Contour: experimental, continuous line; reconstructed by addition of band components, dashed line.

component bands in the 1700 and 1600 cm^{-1} region; however, seven component bands are found in the spectra of the samples in dried films. The positions of the bands identified are quite similar for both samples in solution (H_2O and D_2O) (Table 1), although the peaks of the absorption bands measured in H_2O were found to be generally slightly higher than those in D_2O, as has been described for other proteins (Surewicz & Mantsch, 1988). The positions of the peaks show greater differences in the case of the dried samples and these differences are more significant between 1630 and 1650 cm^{-1} (see Table 1). An analogous FTIR study of another integral membrane protein, mitochondrial cytochrome *c* oxidase, also showed the presence of eight major bands in the amide I region with positions very similar to the ones observed for the PSII RCs (Arrondo et al., 1994; Echabe et al., 1995).

The assignment of the amide I component bands to specific conformational structures is tenable for bands that can be unambiguously assigned. The band around 1658 cm^{-1} corresponds to α-helix plus unordered peptide segments in H_2O but only to α-helix in D_2O. This main band is clearly shown in the decomposed band contours (see Figure 1) and represents about 40% of the secondary structure of PSII RC. The conservation of the 1658 cm^{-1} band in the dried samples seems to indicate that the α-helix structure constitutes the core of the RC integrated in the membrane and independent of the aqueous medium. In the 1640−1620 cm^{-1} region, two different bands that correspond to β-structures were detected, one around 1636 cm^{-1} which arises clearly from intramolecular carbonyl vibrations of β-sheets, and another around 1626 cm^{-1} which can be attributed to β-strands. The quantification indicates the presence of about 10% β-sheet in the hydrated samples. The alteration of the 1636 cm^{-1} band in the dried films suggests that the β-sheets are affected by dehydration. The band around 1626 cm^{-1} has been assigned in other infrared studies (Arrondo et al., 1994) to peptides in an extended configuration, with a hydrogen-bonding pattern formed by peptide residues not taking part in intramolecular β-sheets but rather hydrogen-bonded to other molecular structures, even forming intermolecular monomer-monomer interactions. This kind of configuration is called β-strand or extended chain and is expected to be present in multisubunit complexes, like PSII RC, consisting of several intimately associated proteins with significant regions of the polypeptidic chains outside the transmembrane helices. The quantitative analysis attributes about 14% to extended chain (β-strands) for the samples in H_2O. A possible effect of the dehydration upon the 1626 cm^{-1} band may occur, since its signal decreases about 3−4% in the dried films.

Absorption bands associated with turns (usually β-turns) are located in the 1690−1665 cm^{-1} region, and in this part, the IR spectra of the RCs showed one band at around 1685 cm^{-1} and another at 1674 cm^{-1}. The general contribution of these two bands corresponds to about 17% in the integrated area of the samples in H_2O. When the samples are transferred to D_2O, part of this signal moves to lower vibrational modes, like the one at 1636 cm^{-1} (≈3% increase). This also occurs in cytochrome *c* oxidase (Arrondo et al., 1994).

The assignement of the 1643 cm^{-1} band to a specific protein structural element or motif is, so far, not very clear. The possibility that part of this band is contributed by residual water could be considered, but we ruled this out since the use of different protein concentrations in the FTIR analysis did not give significant variations in the proportion of this band. This indicates that the 1643 cm^{-1} band comes from some structural element that is intrinsic to the protein, independent of the amount of water. Moreover, the 1643 cm^{-1} band was also detected in the samples in D_2O. For intrinsic membrane proteins, it can be assumed that the 1643 cm^{-1} band contains contributions from nonstructured conformations, including mainly open loops, i.e. loops fully hydrated and not interacting with nearby amide functional groups (Fabian et al., 1992). These loops are different from unordered segments, since it has been shown that the loops have a specific tertiary structure while the unordered segments only interact with the solvent (Susi, 1969). The 1643 cm^{-1} band could also be attributed to a coiled-coil conformation, but this structural element is usual in filament proteins and is not commonly present in integral membrane proteins (Reisdorf & Krimm, 1996). Another possibility is that this band was due to certain coupling or interaction between proximate transmembrane α-helices in integral membrane proteins, though this assignment has not been well established. The quantitative analysis of the 1643 cm^{-1} band indicates a significant contribution from this structural

Table 1: Values Corresponding to Peak Position and Percentage Area Obtained after Decomposition of the Amide I Band of Photosystem II Reaction Centers, Measured at Room Temperature in H_2O, D_2O, and Dried Films[a]

H_2O		D_2O		film		main assigments		
peak position (cm^{-1})	area (%)	peak position (cm^{-1})	area (%)	peak position (cm^{-1})	area (%)	band[b,c]	secondary structure	relative amount[d] (%)
1693.4 ± 0.5	0.88 ± 0.08	1694.0 ± 0.7	0.07 ± 0.02	1692.4 ± 0.1	0.68 ± 0.22			
1685.0 ± 0.1	5.02 ± 0.30	1683.2 ± 0.3	3.84 ± 0.19	1683.9 ± 0.3	7.40 ± 0.50	1685,1674	turns	17
1674.4 ± 0.2	12.32 ± 0.59	1673.6 ± 0.1	7.39 ± 0.50	1675.1 ± 0.1	14.42 ± 0.96	1658	α-helix	40
1657.8 ± 0.3	42.94 ± 0.69	1657.7 ± 0.1	39.88 ± 0.44	1658.2 ± 0.1	46.03 ± 0.52	1658	unordered segments	3
1643.9 ± 0.2	14.94 ± 1.26	1643.4 ± 0.1	22.92 ± 1.08	1639.8 ± 0.3	21.96 ± 0.90	1643	loops	15
1636.0 ± 0.3	10.06 ± 0.73	1636.8 ± 0.2	13.02 ± 0.88			1636	*β*-sheet	10
1626.0 ± 0.1	14.08 ± 0.46	1625.4 ± 0.1	12.87 ± 0.54	1627.3 ± 0.1	9.49 ± 0.74	1626	extended chains (*β*-strand)	14
1612.9 ± 0.5		1610.9 ± 0.5		1614.0 ± 0.3				

[a] The data in the first three boxes correspond to the average of three different samples ± the standard deviations. The areas located below 1615 cm^{-1} in the amide I have not been considered in the percentage of area because they correspond to side chain contributions. [b] Characteristic positions of the main bands in H_2O. [c] The width at half-height of all the individual bands assigned between 1690 and 1620 cm^{-1} was in the range between 15 and 20 cm^{-1}. The only exception to this corresponded to the 1640 cm^{-1} band found in the dried films, which showed a width of 22.5 cm^{-1}. By contrast, the bands detected for the samples in H_2O at both sides of that band, at 1643 and 1636 cm^{-1}, showed a width of 18.5 and 18.0 cm^{-1}, respectively. Such an increase in the width at 1640 cm^{-1} may reflect an overlapping of the two vibrational bands assigned to loops and *β*-sheet after the dehydration. The resolution of the FTIR method is 2 cm^{-1} and if both bands move 3−4 cm^{-1} closer because of the dehydration, they will be seen as a single signal. [d] Estimation of the approximate relative amount of each secondary structural element in the isolated PSII RC protein complex.

element, which represents about 15% for the samples in H_2O. Deuteration of the samples induces an increase of the 1643 cm^{-1} band till about 23%, due to inclusion of the signal coming from unordered segments (≈3%) and to incorporation of part of the signal attributed to turns in water solution (≈4−5%). This effect also occurs in other proteins (Surewicz & Mantsch, 1988).

In the films, the drying of the samples affects the 1643 cm^{-1} band, which most probably suffers a displacement to overlap with the 1636 cm^{-1} band, giving an intermediate band at about 1640 cm^{-1}. So this new band that appears in the dried films can be attributed to the modification of the vibrational modes of some structural elements by the dehydration. The drying seems to affect mainly loops and *β*-sheets which are structural elements that interact with water, and their assigned bands in aqueous medium are bands at both sides of 1640 cm^{-1}. The quantification of the 1640 cm^{-1} band shows a proportion of about 22% (Table 1), and the bands at 1643 and 1636 cm^{-1} for the samples in H_2O represent a comparable 25% (15% + 10%). The increase to 22.5 cm^{-1} of the width (at half-height) of the 1640 cm^{-1} band in the films is also indicative of an overlapping (see Table 1). A similar tendency to overlap of the bands corresponding to nonregular structure and *β*-structure has been recently described in a FTIR structural study of tyrosine hydrosylase (Martinez et al., 1996).

The component at around 1693 cm^{-1} in the H_2O spectra is due to the high-frequency band of the antiparallel *β*-sheet and shifts to a lower wavenumber in the D_2O medium. This band represents, in either case, less than 1% of the total percentage. Finally, the band at around 1612 cm^{-1} in the amide I corresponds to side chain contributions, and for this reason, it has not been considered in the quantitative analysis.

Study of Thermal Stability. Protein thermal denaturation profiles are sensitive tools revealing minor conformational differences that are not always apparent from the individual infrared spectra (Arrondo et al., 1994; Taneva et al., 1995). Figure 2 shows a series of IR spectra of PSII RCs obtained in the temperature range from 20 to 80 °C. The changes show a typical pattern of protein thermal denaturation, where two main bands around 1686 and 1622 cm^{-1} arise in the D_2O IR spectra above 50 °C. These bands are clearly observed in the deconvolved spectra (Figure 2b) and are slightly shifted to higher wavenumbers (1695 and 1627 cm^{-1}) for the samples in H_2O (spectra not shown). These bands are characteristic of protein aggregation produced after irreversible thermal denaturation and have been described for both soluble and membrane proteins (Jackson & Mantsch, 1995). Apart from these signals present in the higher-temperature range (i.e. above 50 °C), the study of the PSII RCs shows a major change of the IR spectra in the temperature range between 40 and 45 °C. This thermally induced modification can be clearly observed when the width of the amide I band at half-height is plotted against temperature. Figure 3 shows this graphic representation as a sigmoidal curve where the band width increases with the temperature from 25 to 65 °C. The isosbestic point of the sigmoidal curve occurs at 42.5 °C and can be considered to be a main and distinct thermal transition in the IR spectra of the PSII RCs. Since FTIR reflects the secondary structure of the PSII RCs, figure 3 indicates the existence of a conformational change induced by heat in this protein complex. The relative lowly temperature of this transition compared with the main thermal transitions of other membrane proteins (Arrondo et al., 1994; Taneva et al., 1995) reflects a high thermal instability of the PSII RC complex. Although photochemical activity assays were not carried out over the whole temperature range, measurements at 45 °C indicated a complete loss of activity. This loss of enzyme activity was irreversible.

DISCUSSION

It is usually assumed from structural predictions that all five proteins of the isolated PSII RC contain transmembrane segments which are α-helices. Analysis of multiple sequences of the D1/D2 heterodimer from more than 15 different plants has allowed the construction of a predicted folding pattern which includes five transmembrane α-helices for D1 and five α-helices for D2 (Svensson et al., 1990, 1991). Moreover, predictions indicate that D1 and D2 have two surface α-helices each: one stromal, between transmembrane segments 4 and 5 (around Q_A and Q_B binding sites), and another lumenal, between transmembrane segments 3 and 4. These could contain around 10 amino acids each (i.e. 20 for both surface helices). The number of amino acids from D1/D2 included in the 10 transmembrane

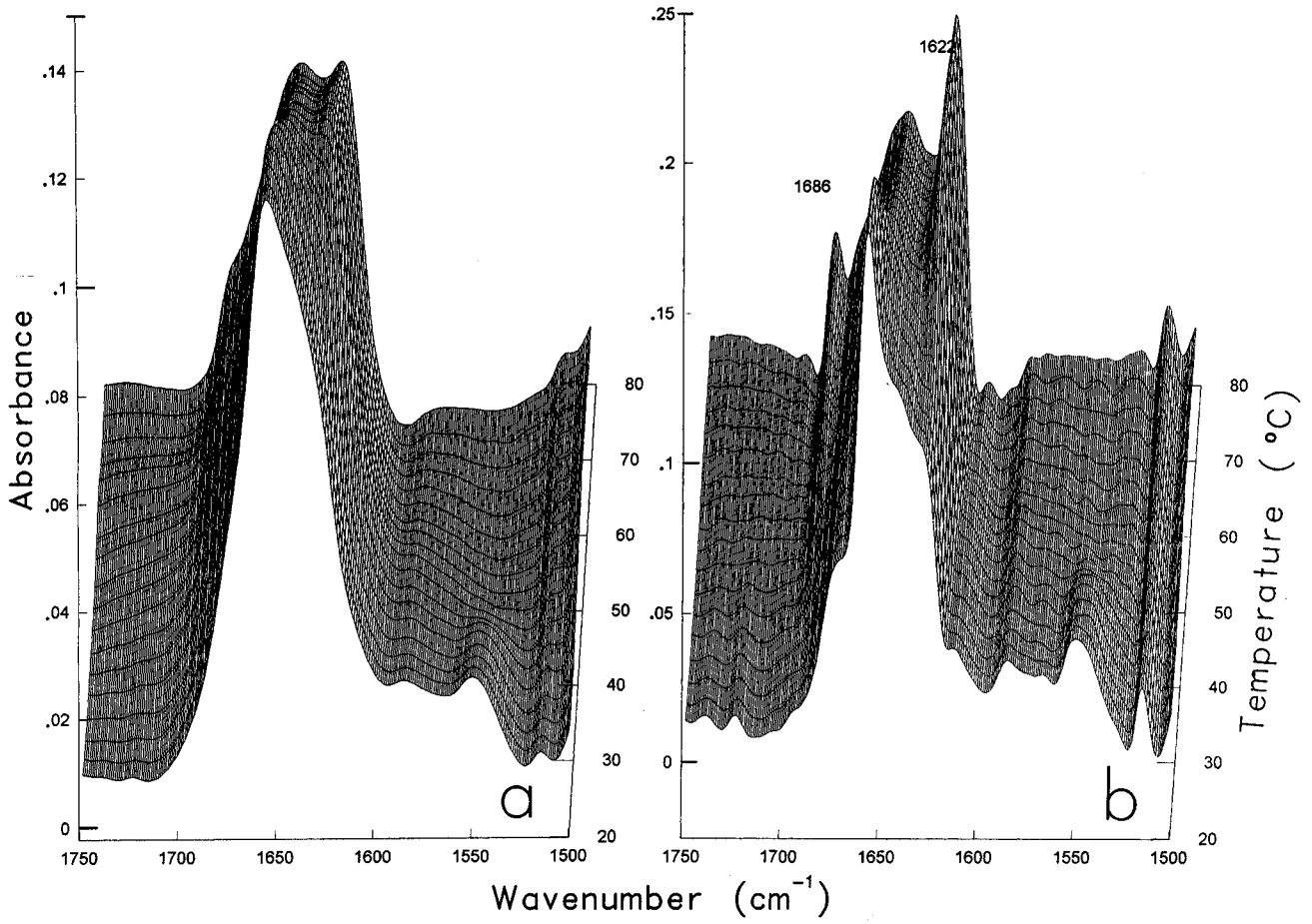

FIGURE 2: Infrared spectra (for the 1750−1500 cm^{-1} region) of the PSII RCs in D_2O buffer as a function of temperature: original spectra (a) and deconvolved spectra (b). The deconvolution parameters were a band width of 18 cm^{-1} and an enhancement factor (*K*) of 2. The temperature is represented as a third dimension with a small angle over the *X*/*Y* plane. The first spectra correspond to a temperature of 25 °C, and 17 steps are represented with an increment of about 3 °C, till 75 °C for the last spectra. Note the appearance of bands 1686 and 1622 cm^{-1} when the temperature increases.

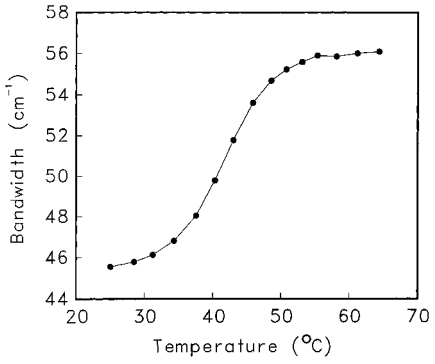

FIGURE 3: Thermal profile of the amide I bandwidth of the PSII RCs in D_2O buffer at half of its height from 25 to 65 °C. The band width is calculated at half-height of the maximum peak between 1600 and 1700 cm^{-1}. Above 65 °C, there is a significant loss of absorbance by the protein.

α-helices is predicted to be 119 out of 344 for D1 and 120 out of 353 for D2 (Svensson et al., 1996). Similar amino acid analysis and comparison of multiple sequences of cytochrome b_{559} have indicated that this protein consists of two transmembrane α-helices, one in each subunit, that include 26 amino acids out of 82 for the α subunit and 25 out of 39 for the β subunit (Tae & Cramer, 1994). Finally, the *Psb*I protein is also predicted to contain a membrane-spanning segment with a putative α-helix structure where 22 amino acids out of 36 are included (Ikeuchi & Inoue, 1988). From all these data, it can be calculated that, as a whole, 352 amino acids of the PSII RC are located in segments of α-helix structure. This figure represents 41.2% of the total of 854 amino acids of the RC. This percentage is in good agreement with the amount of α-helix structure in the isolated RCs calculated by FTIR reported here. From these figures, it can also be inferred that the amount of polypeptide chain located between the transmembrane segments in the PSII RCs is very significant (about 60% of the total). These major polypeptidic sections have a more hydrophilic character and, except for the two proposed surface helices of the D1 and D2 proteins, will have other secondary structures like β-sheets, β-strands, turns, and loops.

The above considerations have a major consequence for the drawing of a current structural model of PSII; we can not restrict our view of this protein complex to a main core of about a dozen α-helices buried in the thylakoid membrane connected by small loops. This is the idea on which the theoretical models of PSII are based (Svensson et al., 1990, 1996; Ruffle et al., 1992), and it comes from an understandable but excessive attempt to make a homologous comparison of the PSII RCs with the well-resolved crystal structure of the purple bacteria photosynthetic RCs (Deisenhofer et al., 1985; Allen et al., 1987). If we follow this idea of homology, we could, for example, expect a clear predominance of α-helix in the secondary structure of PSII RC, as it happens with the L/M heterodimer of the bacterial RCs: 64% (Deisenhofer et al., 1985) and 66% (Allen et al., 1987). In this respect, the first structural analysis of PSII RCs by FTIR using comparison with standard proteins gave 67.2% α-helix

structure (He et al., 1991). Our reevaluation of this data, using a different FTIR quantitative method, gives a lower percentage (40%) more consistent with an analysis of the amino acid hydrophobic pattern of the PSII RC (as discussed above) and with the current models of the architecture of PSII (as discussed below). The fact that a similar disagreement was found in the FTIR studies of cytochrome *c* oxidase is worth mentioning (Arrondo et al., 1994), since the 39−41% α-helix content determined by the same method used in this paper contrasted with the 61% obtained by a different IR quantitative method (Dong et al., 1990). The crystal structure of this oxidase has confirmed a content of about 40% α-helix (Iwata et al., 1995; Tsukihara et al., 1996). Part of this discrepancy, found by the use of different quantitative methods based on FTIR spectroscopy, could also be due to the existence of certain signals from coupling between α-helices that have still not been well assigned and characterized.

A FTIR study including band decomposition and quantitative analysis similar to that described here for dried films of PSII RCs was reported for films of bacterial reaction centers (including L, M, H, and C subunits) (Nabedryk et al., 1991). In this work, the authors determined three main secondary structural elements: β-turns, α-helix, and β-structure assigned to the bands at ≈1680, ≈1658, and ≈1638 cm^{-1}, respectively. They indicated that the air-dried film may lead to an overestimation of the β-sheet, since they determined a content of 20−25% β-sheet corresponding to the 1638 cm^{-1} band. This effect is similar to the one we see in Table 1 if we only consider the data from the films, where the 1639 cm^{-1} band represents 22% of the area. However, our data from samples in H_2O and D_2O allow us to distinguish two different bands around 1640 cm^{-1} which most probably overlap after the drying.

A detailed study of the conserved amino acid sequence of the D1 protein outside the transmembrane segments shows that two big loops (of 52 and 30 amino acids) and the C-terminal long chain (of 51 amino acids) come out of the core of five predicted α-helices toward the lumen side (Svensson et al., 1991). The same occurs for the D2 protein which is analogous to D1. From these data, it can be suggested that these large portions of the polypeptide chains should clearly protrude out of the plane of the thylakoid membrane where PSII is anchored. The significant proportion of turns (17%), loops (15%), and extended chains (14%) detected by our FTIR structural analysis is consistent with the suggestion that the PSII RCs have important structural elements outside the membrane plane with multiple conformations. At the same time, the sequence analyses of D1 and D2 have shown that these lumenal loops include a significant proportion of charged amino acids and a surprisingly high amount of Gly and Pro conserved residues (Svensson et al., 1990). The presence of charged amino acids brings about the possibility of hydrostatic interactions with other proteins, while the presence of Gly and Pro probably restricts the formation of estensive surface α-helices, since this secondary structure is not favored by such amino acids.

The recent low-resolution 3D images of the PSII complex obtained by electron mycroscopy and digital image processing of 2D crystals (Holzenburg et al., 1993; Santini et al., 1994; Morris et al., 1997) and of isolated particles (Boekema et al., 1995) have shown that most of PSII is exposed to the lumen and comes out of the 4.5 nm thick membrane bilayer. These studies have calculated an overall height of the PSII complex of around 9 nm, excluding the three extrinsic proteins (33, 23, and 17 kDa) that stabilize the oxygen-evolving cluster and which are not in isolated PSII RCs. These observations indicate again the structural significance of the extramembrane part of the PSII RC. Recent studies have shown that D1 participates in the formation of the lumenal oxygen-evolving binding site associated with the 33 kDa extrinsic protein (Eisenberg-Domovich et al., 1995) and that the first lumenal loop of the D1 protein is important for the assembly of the PSII complex (Dalla Chiesa et al., 1996). The determination of the secondary structure of this 33 kDa extrinsic protein of PSII by FTIR (Ahmed et al., 1995) has shown that the main structural component of this polypeptide is 36% β-sheet. These β-sheets could interact with the β-sheet structure that we have detected in the RCs (10%), forming a possible domain of contact and adhesion with the extrinsic parts of PSII on the lumenal side of the complex.

A good complement to any study on the secondary structure of a protein is the analysis of its thermal stability. The internal thermodynamic parameters of a certain protein are linked to its specific structure and conformation, and any change in these parameters will induce detectable conformational changes. FTIR is a very appropiate technique for visualizing changes in conformation induced by temperature. The thermal denaturation of the PSII complex has been investigated previously by differential scanning calorimetry (DSC) (Cramer et al., 1981; Thompson et al., 1986; 1989; Shutilova et al., 1995). The first study, done using PSII-enriched membranes, showed a complex pattern of heat denaturation with five major DSC peaks corresponding to five endothermic transitions detected between 30 and 70 °C (Thompson et al., 1986). These peaks were assumed to correspond to five independent denaturation steps of the samples, and the peak at ≈48 °C was assigned to the functional denaturation of the PSII oxygen-evolving complex. This had been also suggested by DSC scans of thylakoid membranes, where a transition at 42−44 °C was observed (Cramer et al., 1981). A more recent DSC study has found that the temperature of semi-inactivation of oxygen evolution was 45 °C for PSII-enriched membranes and 34 °C for PSII oxygen-evolving cores (Shutilova et al., 1995). All the studies mentioned above propose that the thermoinactivation of oxygen evolution of PSII comes from a modification of the manganese cluster that induces Mn^{2+} release. Our present study on thermal stability is made on isolated PSII RCs that do not evolve oxygen and where the manganese cluster is not bound. However, our results also show a distinct thermal transition with a half-point at 42.5 °C that correlates quite well with the transition attributed to the inactivation of oxygen evolution. The D1 and D2 polypeptides constitute the active nucleus of PSII and are the main proteins that link and sustain the manganese cluster (Chu et al., 1995). A structural change in these polypeptides will therefore be expected to affect substantially the binding, conformation, and function of this cluster.

A high thermal sensitivity of the secondary structure of PSII is in good agreement with the well-described instability of this protein complex (Barber & Andersson, 1992). Such instability is caused by the fact that PSII is the molecular target of the physiological process of photoinhibition which occurs in plants. Under situations of high light illumination and metabolic stress, plants suffer the impairment of their photosynthetic activity, and they become photoinhibited. The

PSII RC is the main weak point affected by this impairment, and the gradual alteration of the PSII RCs has been shown to start with pigment bleaching (Telfer et al., 1991) and end with proteolytic degradation of the central D1 polypeptide (De Las Rivas et al., 1993). The detection of thermoinduced conformational changes in PSII RCs by FTIR gives a hint of the mechanism whereby a structural change of the RC could be the protein signal needed for the specific degradation by proteases. The thermally induced structural change, which we observe *in vitro*, may also be induced by other means, such as photodamage, when PSII is functioning photochemically *in vivo*. More detailed studies on the structure and function of PSII by different techniques have to be carried out in order to better elucidate how certain specific conformational changes of some domains of the polypeptides of PSII can modify its activity.

ACKNOWLEDGMENT

We sincerely thank Dr. Jose Luis R. Arrondo and Dr. Arturo Muga for valuable guiding in the use of the FTIR spectroscopy and for advice and help in the analyses of the results. We are also grateful to Izaskun Echabe for helping with the handling of the computers.

REFERENCES

Ahmed, A., Tajmir-Riahi, H. A., & Carpentier, R. (1995) *FEBS Lett. 363*, 65−68.
Allen, J. P., Feher, G., Yeates, T. O., Komiya, H., & Rees, D. C. (1987) *Proc. Natl. Acad. Sci. U.S.A. 84*, 6162−6166.
Arrondo, J. L. R., Muga, A., Castresana, J., Bernabeu, C., & Goñi, F. M. (1989) *FEBS Lett. 252*, 118−120.
Arrondo, J. L. R., Muga, A., Castresana, J., & Goñi, F. M. (1993) *Prog. Biophys. Mol. Biol. 59*, 23−56.
Arrondo, J. L. R., Castresana, J., Valpuesta, J. M., & Goñi, F. M. (1994) *Biochemistry 33*, 11650−11655.
Bañuelos, S., Arrondo, J. L. R., Goñi, F. M., & Pifat, G. (1995) *J. Biol. Chem. 270*, 9192−9196.
Barber, J. (1994) *Biochem. Soc. Trans. 22*, 313−318.
Barber, J., & Andersson, B. (1992) *Trends Biochem. Sci. 17*, 61−66.
Boekema, E. J., Hankamer, B., Bald, D., Kruip, J., Nield, J., Boonstra, A. F., Barber, J., & Rogner, M. (1995) *Proc. Natl. Acad. Sci. U.S.A. 92*, 175−179.
Chapman, D. J., Gounaris, K., & Barber, J. (1988) *Biochim. Biophys. Acta 933*, 423−431.
Chu, H. A., Nguyen, A. P., & Debus, R. J. (1995) *Biochemistry 34*, 5839−5858.
Cramer, W. A., Whitmarsh, J., & Low, P. S. (1981) *Biochemistry 20*, 157−162.
Dalla Chiesa, M., Deak, Z., Vass, I., Barber, J., & Nixon, P. (1996) *Photosyn. Res. 50*, 79−91.
De Las Rivas, J., Shipton, C. A., Ponticos, M., & Barber, J. (1993) *Biochemistry 32*, 6944−6950.
Deisenhofer, J., Epp, O., Miki, K., Huber, R., & Michel, H. (1985) *Nature 318*, 618−624.
Dekker, J. P., Betts, S. D., Yocum, C. F., & Boekema, E. J. (1990) *Biochemistry 29*, 3220−3225.
Dong, A., Huang, P., and Caughey, W. S. (1990) *Biochemistry 29*, 3303−3308.
Echabe, I., Haltia, T., Freire, E., Goñi, F. M., & Arrondo, J. L. R. (1995) *Biochemistry 34*, 13565−13569.
Eisenberg-Domovich, Y., Oelmuller, R., Herrmann, R. G., & Ohad, I. (1995) *J. Biol. Chem. 270*, 30181−30186.
Fabian, H., Naumann, D., Misselwitz, R., Ristau, O., Gerlach, D., & Welfle, H. (1992) *Biochemistry 31*, 6532.
Haris, P. I., & Chapman, D. (1993) *Biochem. Soc. Trans. 21*, 9−15.
He, W.-Z., Newell, W. R., Haris, P. I., Chapman, D., & Barber, J. (1991) *Biochemistry 30*, 4552−4559.
Holzenburg, A., Bewley, M. C., Wilson, F. H., Nicholson, W. V., & Ford, R. C. (1993) *Nature 363*, 470−472.
Ikeuchi, M., & Inoue, Y. (1988) *FEBS Lett. 241*, 99−104.
Iwata, S., Ostermeier, C., Ludwig, B., & Michel, H. (1995) *Nature 376*, 660−669.
Jackson, M., & Mantsch, H. H. (1995) *Crit. Rev. Biochem. Mol. Biol. 30*, 95−120.
Krauss, N., Hinrichs, W., Witt, I., Fromme, P., Pritzkow, W., Dauter, Z., Betzel, C., Wilson, K. S., Witt, H. T., & Saenger, W. (1993) *Nature 361*, 326−331.
Krimm, S., & Bandekar, J. (1986) *Adv. Protein Chem. 38*, 181−364.
Lee, D. C., Haris, P. I., Chapman, D., & Mitchell, R. C. (1990) *Biochemistry 29*, 9185−9193.
Lyon, M. K., Marr, K. M., & Furcinitti, P. S. (1993) *J. Struct. Biol. 110*, 133−140.
Marr, K. M., Mastronarde, D. M., & Lyon, M. K. (1996) *J. Cell. Biol. 132*, 823−833.
Martínez, A., Haavik, J., Flatmark, T., Arrondo, J. L. R., & Muga, A. (1996) *J. Biol. Chem. 271*, 19737−19742.
Morris, E. P., Hankamer, B., Zheleva, D., Friso, G., & Barber, J. (1997) *Structure* (in press).
Nabedryk, E., Breton, J., & Thibodeau, D. L. (1991) in *Spectroscopy of Biological Molecules* (Hester, R. E., & Girling, R. B., Eds.) pp 67−68, The Royal Society of Chemistry, Herts, England.
Nakazato, K., Toyoshima, C., Enami, I., & Inoue, Y. (1996) *J. Mol. Biol. 257*, 225−232.
Nicholson, W. V., Shepherd, F. H., Rosenberg, M. F., Ford, R. C., & Holzenburg, A. (1996) *Biochem. J. 315*, 543−547.
Reisdorf, W. C. J., & Krimm, S. (1996) *Biochemistry 35*, 1383−1386.
Ruffle, S. V., Donnelly, D., Blundell, T. L., & Nugent, J. H. A. (1992) *Photosynth. Res. 34*, 287−300.
Santini, C., Tidu, V., Tognon, G., Ghiretti-Magaldi, A., & Bassi, R. (1994) *Eur. J. Biochem. 221*, 307−315.
Shutilova, N., Semenova, G., Klimov, V., & Shnyrov, V. (1995) *Biochem. Mol. Biol. Int. 35*, 1233−1243.
Surewicz, W. K., & Mantsch, H. H. (1988) *Biochim. Biophys. Acta 952*, 115−130.
Susi, H. (1969) in *Structure and Stability of Biological Macromolecules* (Timasheff, S. N., & Stevens, L., Eds.) pp 575−663, Marcel Dekker, New York.
Svensson, B., Vass, I., Cedergren, E., & Styring, S. (1990) *EMBO J. 9*, 2051−2059.
Svensson, B., Vass, I., & Styring, S. (1991) *Z. Naturforsch. C 46*, 765−776.
Svensson, B., Etchebest, C., Tuffery, P., van Kan, P., Smith, J., & Styring, S. (1996) *Biochemistry 35*, 14486−14502.
Tae, G.-S., & Cramer, W. A. (1994) *Biochemistry 33*, 10060−10068.
Taneva, S. G., Caaveiro, J. M. M., Muga, A., & Goñi, F. M. (1995) *FEBS Lett. 367*, 297−300.
Telfer, A., De Las Rivas, J., & Barber, J. (1991) *Biochim. Biophys. Acta 1060*, 106−114.
Thompson, L. K., Sturtevant, J. M., & Brudvig, G. W. (1986) *Biochemistry 25*, 6161−6169.
Thompson, L. K., Blaylock, R., Sturtevant, J. M., & Brudvig, G. W. (1989) *Biochemistry 28*, 6686−6695.
Tsiotis, G., Walz, T., Spyridaki, A., Lusting, A., Engel, A., & Ghanotakis, D. (1996) *J. Mol. Biol. 259*, 241−248.
Tsukihara, T., Aoyama, H., Yamashita, E., Tomizaki, T., Yamaguchi, H., Shinzawa-Itoh, K., Nakashima, R., Yaono, R., & Yoshikawa, S. (1996) *Science 272*, 1136−1144.
Walker, J. E., & Saraste, M. (1996) *Curr. Opin. Struct. Biol. 6*, 457−459.

BI970684W